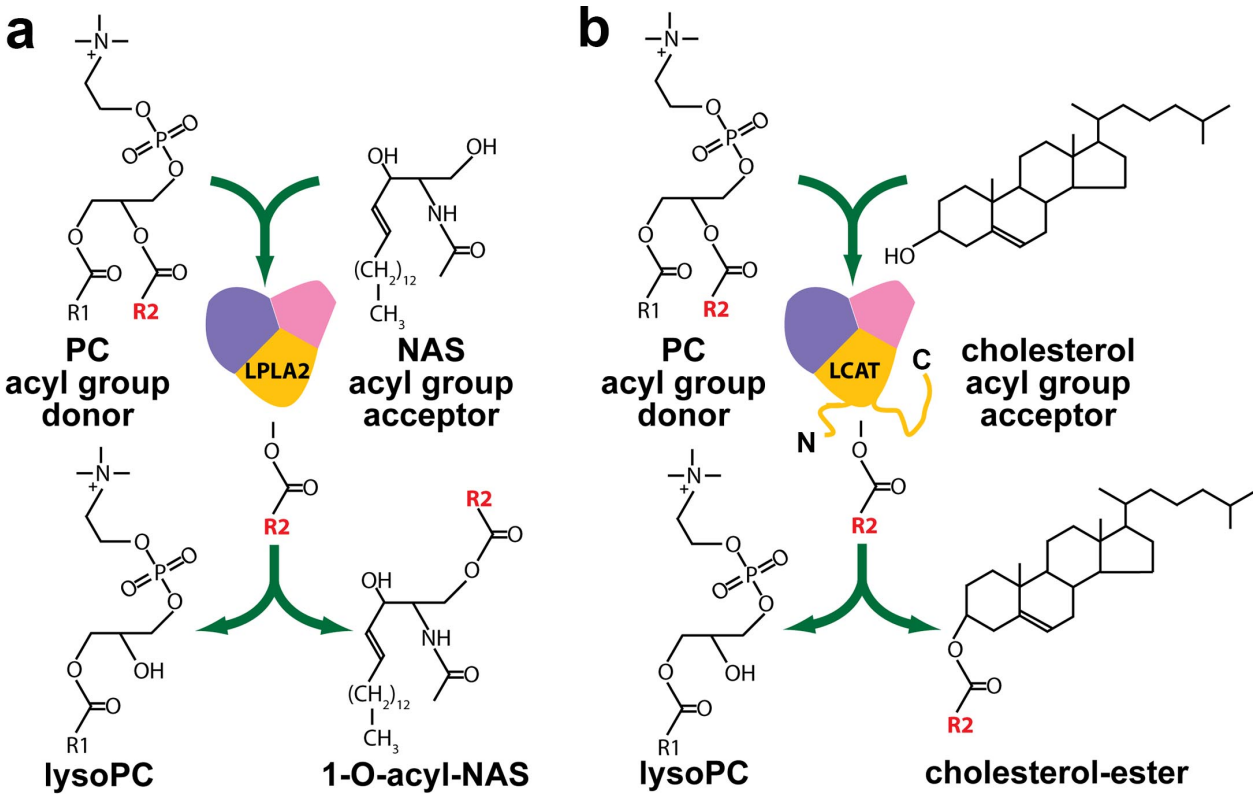

Supplementary Figure 1. Acyltransferase reaction scheme for **(a)** LPLA2 and **(b)** LCAT. PC, phosphatidylcholine; lysoPC, lyso-phosphatidylcholine; NAS, *N*-acetyl-sphingosine; 1-*O*-acyl-NAS, 1-*O*-acyl-*N*-acetyl-sphingosine. Both enzymes preferentially transfer the *sn*-2 acyl chain, and prefer unsaturated fatty acids in this position.

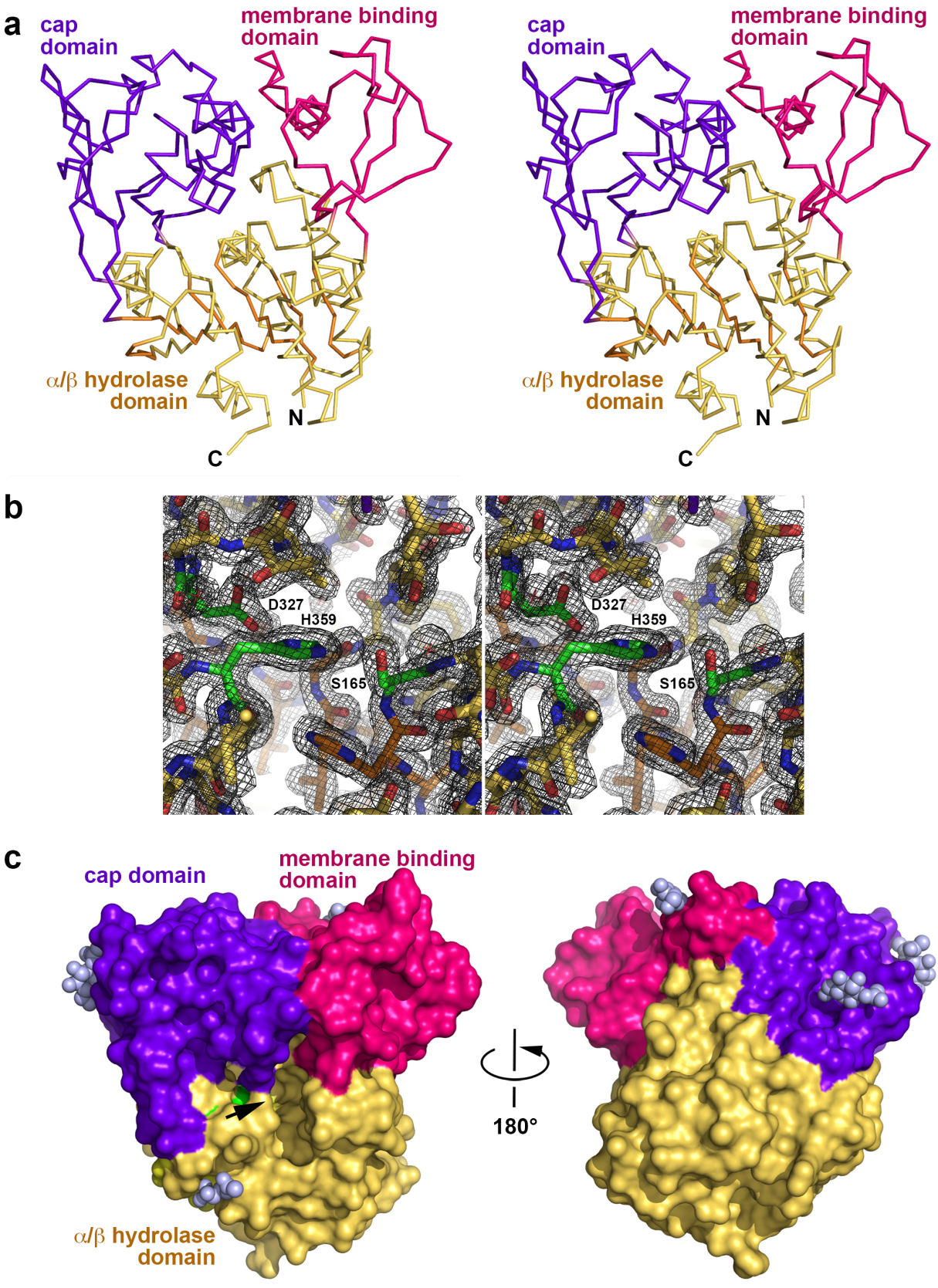
a
cap domain
membrane binding domain
α/β hydrolase domain
N
C
cap domain
membrane binding domain
α/β hydrolase domain
N
C
b
D327
H359
S165
D327
H359
S165
c
cap domain
membrane binding domain
α/β hydrolase domain
180°

Supplementary Figure 2. LPLA2 structure. **(a)** Cross-eyed stereo image of the LPLA2 Cα trace. Domain coloring is as described in Figure 1, and the observed amino and carboxyl terminal residues are labeled N and C, respectively. **(b**) Stereo image of the active site region in the wild-type ligand-free LPLA2 structure with its corresponding 2Fo-Fc map contoured at 1.5 σ (grey wire cage). **(c)** Surface representation of LPLA2 molecule from the same point of view as in Figure 1 (left) and rotated 180° around vertical axis (right). Arrow indicates the entrance into the active site.

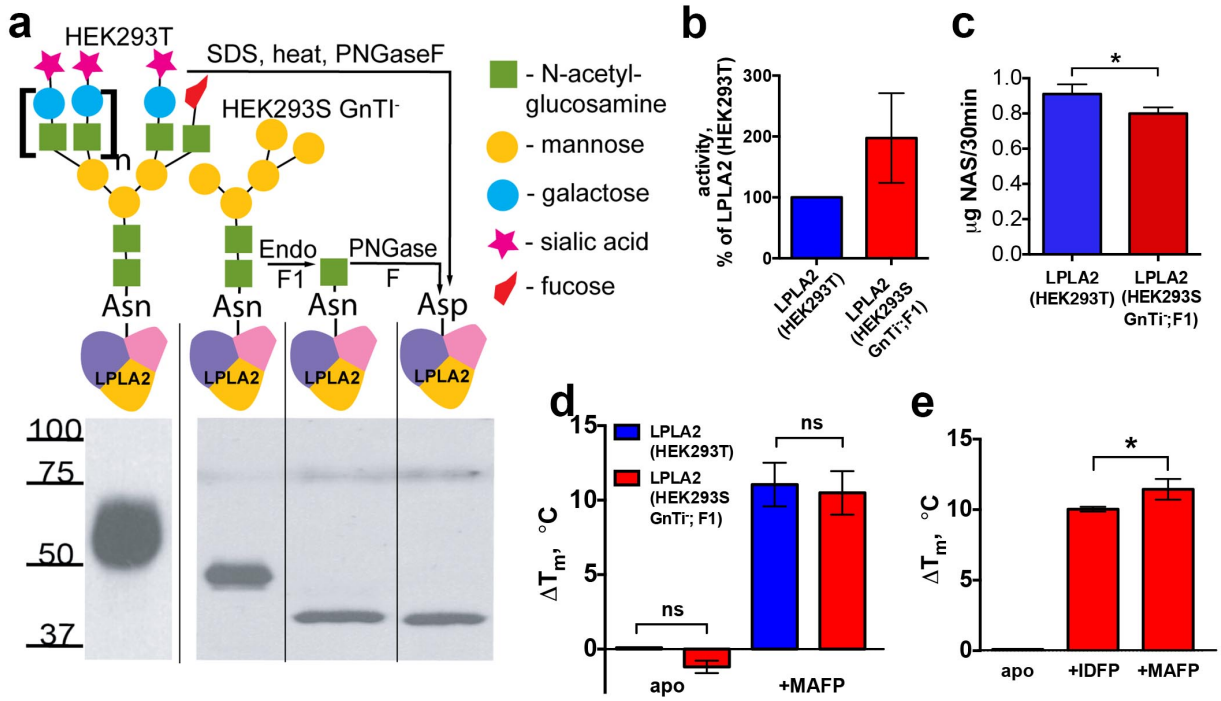

Supplementary Figure 3. Expression, deglycosylation, and covalent modification of LPLA2. **(a)** Coomassie stained gel of various glycosylated forms of LPLA2. The enzyme has four N-linked glycosylation sites that proved resistant to deglycosylation when expressed in HEK293T cells. Crystal structures were obtained for all but the peptide-*N*-glycosidase F (PNGaseF) treated form. **(b)** LPLA2 expressed in HEK293S GnTi$^-$ cells after endoF1 treatment is just as if not more active than wild-type when evaluated using pNPB as a substrate, indicating that deglycosylation of all but the terminal sugar does not greatly affect the structure and function of the enzyme. **(c)** Acyltransferase activity of endoF1-treated LPLA2 is similar to that of wild type. Error bars in panels b and c represent the standard deviation of three independent experiments. **(d)** T_m of LPLA2 expressed in various cell lines before and after reaction with MAFP. **(e)** T_m of endoF1-treated LPLA2 secreted from HEK293S GnTi$^-$ cells after reaction with IDFP or MAFP. In panels d and e, the error bars represent the standard deviation of three independent experiments performed in triplicate. (* $p<0.05$; ns, not significant; Student's t-test)

IDFP

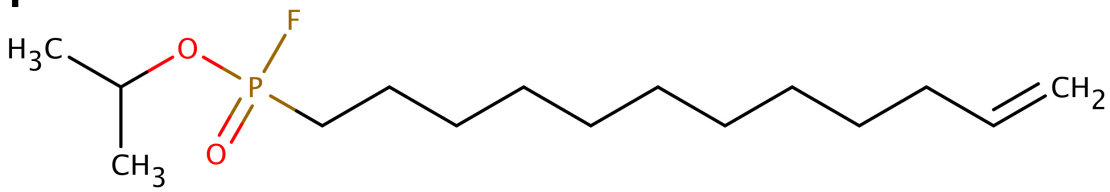

MAFP

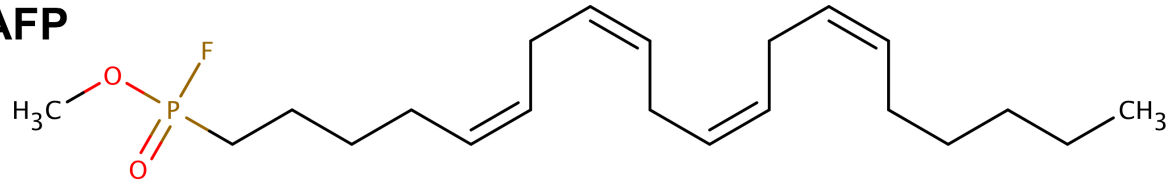

Supplementary Figure 4. Chemical structures of fluoroposphonate inhibitors isopropyl dodec-11-enyl fluorophosphonate (IDFP) and methyl arachidonyl fluorophosphonate (MAFP).

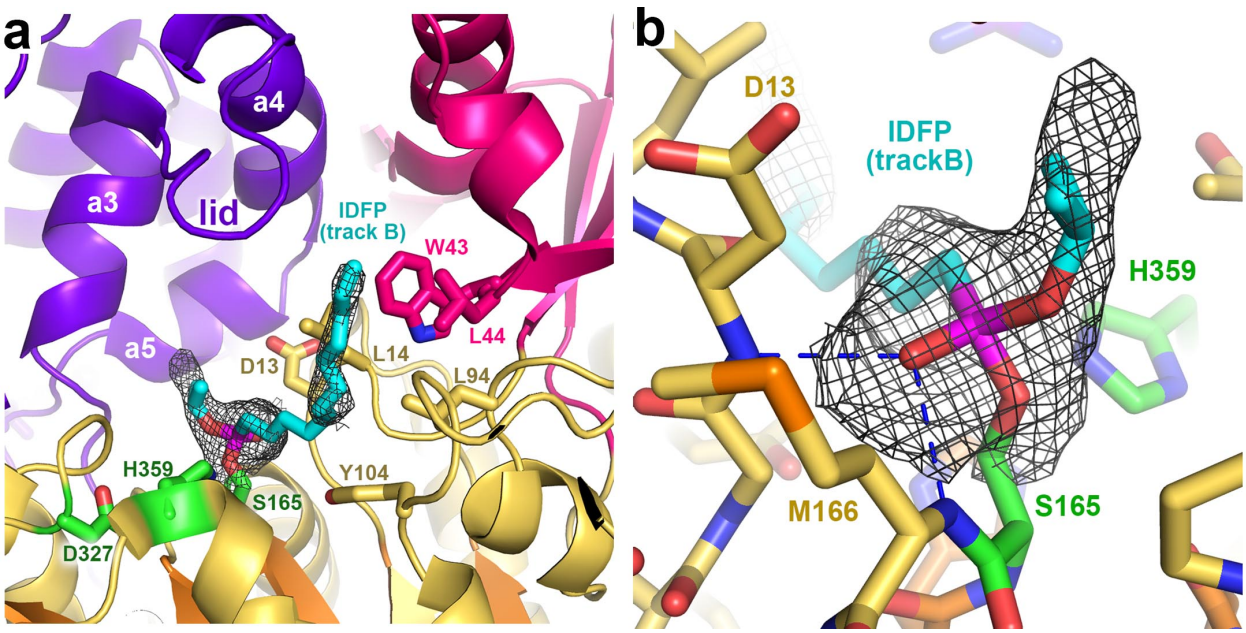

Supplementary Figure 5. IDFP modeled to occupy track B of LPLA2 (*cf.* Fig. 3a). **(a)** IDFP in chains A, B and D of the LPLA2·IDFP structure occupies track B. Residues defining track B are shown as sticks with carbons colored according to their domain assignment as in Figure 1. **(b)** Regardless of the track, the phosphonate of the IDFP head group forms hydrogen bonds (dashed blue lines) with the backbone amides of Asp13 and Met166 comprising the oxyanion hole. Wire cages correspond to 2.5 σ $|F_o|$-$|F_c|$ omit maps.

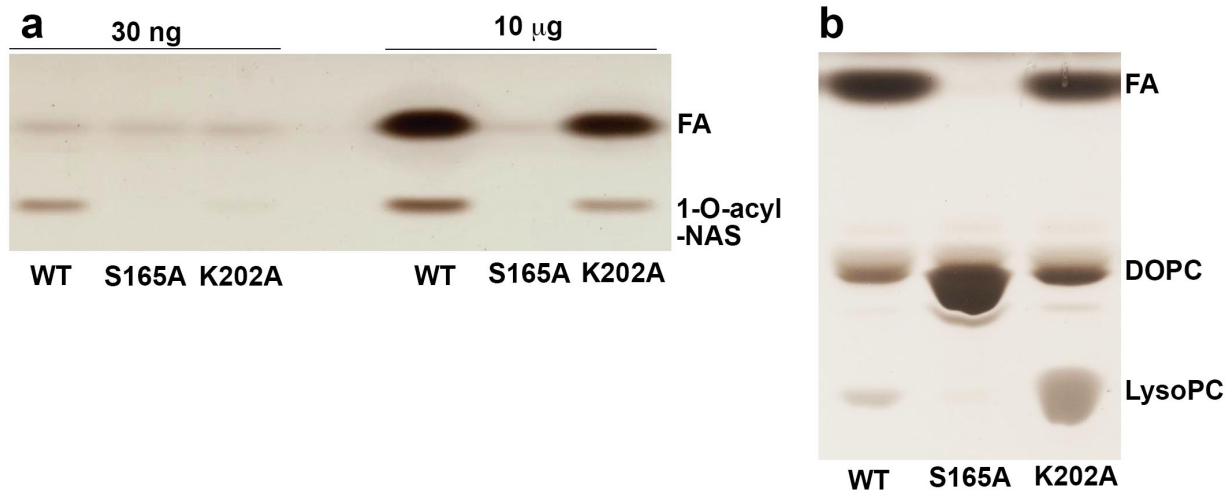

Supplementary Figure 6. The LPLA2-K202A mutation reduces, but does not eliminate LPLA2 catalytic activity. **(a)** Transacylase assay using 3:10:1 molar ratio of NAS-DOPC-sulfatide liposomes. Reaction products relative to the negative control (S165A) are only observed at high enzyme concentrations. FA, fatty acid. **(b)** Esterase assay using (10:1) DOPC-sulfatide liposomes and 10 μg protein. Wild-type (WT) LPLA2 is more efficient at hydrolyzing both DOPC as well as the reaction product lysophosphatidic acid (LysoPC). K202A esterase activity is reduced judged by the amount of DOPC and LysoPC remaining after 30 min as well as by the amount of FA produced.

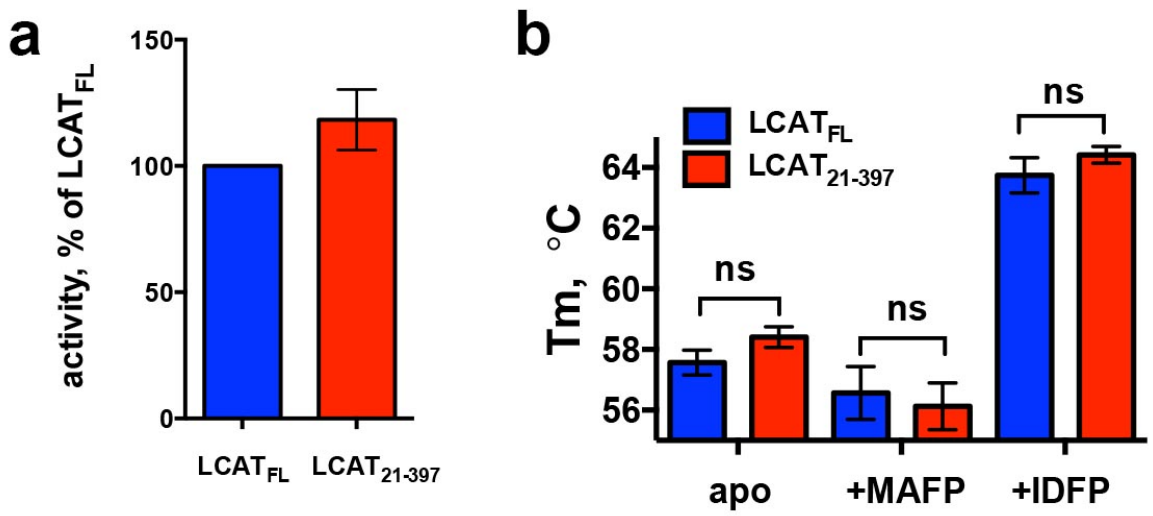

Supplementary Figure 7. Biochemical properties of LCAT variants. **(a)** $LCAT_{FL}$ and $LCAT_{21-397}$ exhibit no significant difference in activity using pNPB as a substrate, indicating that the N and C terminal extensions do not contribute to catalytic activity using soluble substrates. **(b)** T_m values of LCAT variants before and after reaction with MAFP and IDFP. Because treatment with MAFP does not increase the T_m, its longer alkyl chain seems to prevent it from reaction, consistent with the preference of human LCAT for transfer of shorter acyl chains. The error bar represent the standard deviation of three independent experiments performed in triplicate. (ns, not significant; Student's t-test)

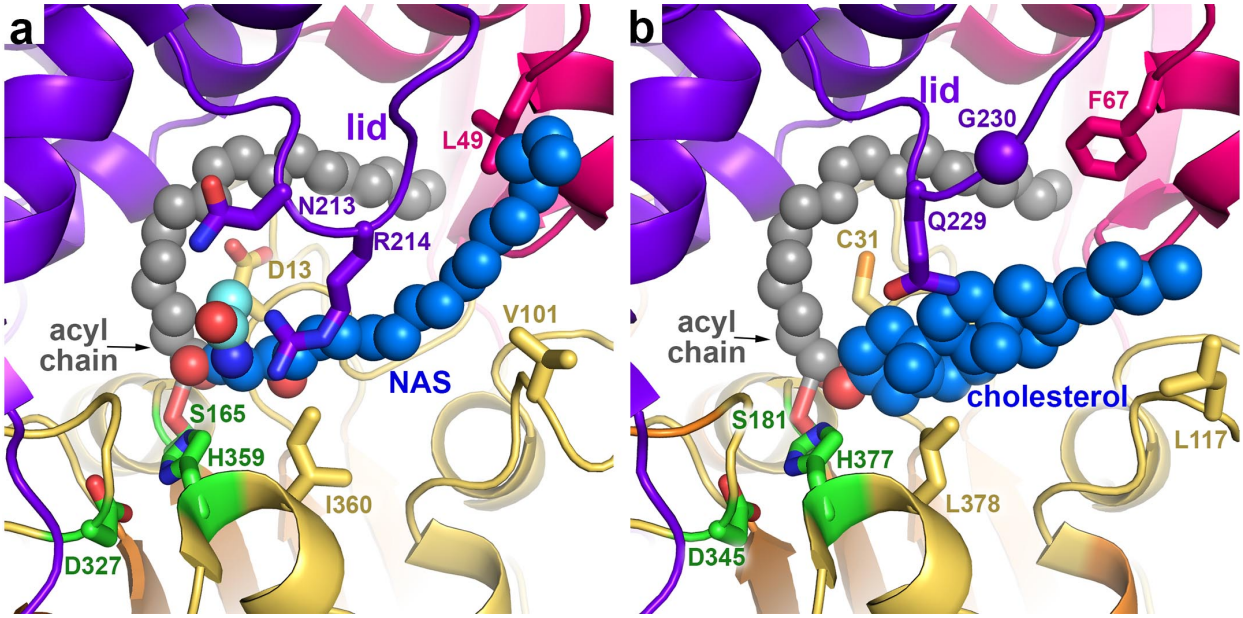

Supplementary Figure 8. Comparison of acyl group acceptors modeled in complex with LPLA2 and LCAT. **(a)** NAS modeled in complex with LPLA2. Arg214 in the lid loop constrains the entrance to the active site near the catalytic triad, which as a result may favor the binding of more slender acceptor substrates. The ceramide side chain (cyan carbons) cannot be long given packing constraints with Asp13. **(b)** Cholesterol modeled in complex with LCAT. The presence of Gly230 (Arg214 in LPLA2) opens up the entrance to track B such that it could more readily accommodate bulkier acyl acceptors. In each panel, side chains of residues in track B that are different between LPLA2 and LCAT are drawn as sticks.

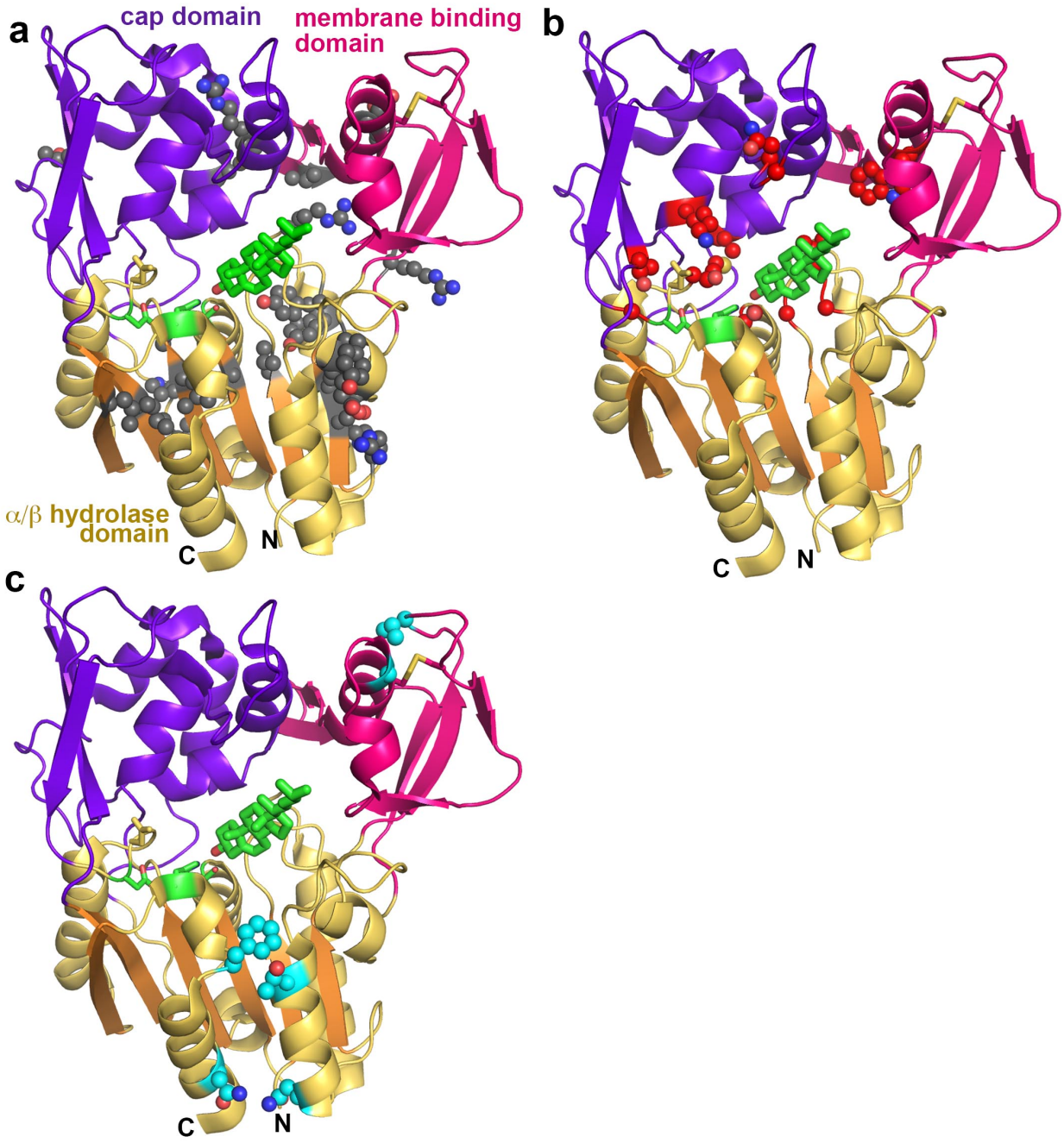

Supplementary Figure 9. Positions mutated in FLD and FED patients mapped onto the structure of LCAT. **(a)** Structural mutations (spheres with grey carbons) most likely cause defects in LCAT folding, stability, and/or sorting. **(b)** Catalytic mutations (spheres with red carbons) most likely interfere with LCAT catalytic functions either by structural perturbation of catalytic residues or by inhibiting substrate binding. **(c)** Mutations that likely interfere either with membrane or HDL binding (spheres with cyan carbons). Cholesterol (stick model with green carbons) is modeled in the active site to indicate the expected acceptor binding site.

Supplementary Table 1. Data collection statistics for SeMet LPLA2

	SeMet LPLA2
Data collection	
Space group	$P\,2_1$
Cell dimensions	
a, *b*, *c* (Å)	91.2 114.3 100.4
α, β, γ (°)	90 102 90
Wavelength (Peak, Å)	0.97937
Resolution (Å)	29.7 – 2.79 (2.94 – 2.79)*
R_{merge}	0.161 (0.529)
I/σ_I	13.0 (5.2)
Completeness (%)	99.2 (95.4)
Redundancy	15.2 (14.5)

Data was collected from a single SeMet LPLA2 crystal.
*Data for highest resolution shell is shown in parentheses.

Supplementary Table 2. Data collection and refinement statistics for glycosylated forms of LPLA2

	LPLA2·MAFP (HEK293S GnTI$^-$)	LPLA2 (HEK293T)
Data collection		
Space group	$P\,6_2\,2\,2$	$P\,2\,2_1\,2_1$
Cell dimensions		
a, *b*, *c* (Å)	96.0 96.0 208.0	72.4 125.3 140.2
α, β, γ (°)	90 90 120	90 90 90
Resolution (Å)	30 – 2.69 (2.82 – 2.69)*	30 – 2.95 (3.13– 2.95)
R_{merge}	0.130 (0.675)	0.214 (1.297)
I/σ_I	16.1 (3.5)	3.1 (0.6)
Completeness (%)	99.7 (98.6)	48.0 (9.6)
Redundancy	12.5 (12.1)	4.5 (4.3)
Refinement		
Resolution (Å)	29.4 – 2.69	30 – 3.08
No. reflections	15534	11420
R_{work}/ R_{free}	0.177/0.221	0.249/0.264
No. atoms		
Protein	3019	6041
Ligand/ion	96	176
Water	34	0
B-factors		
Protein	50.3	152.1
Ligand/ion	79.4	194.3
Water	45.5	
R.m.s deviations		
Bond lengths (Å)	0.01	0.004
Bond angles (º)	1.41	0.924

Each structure was solved using data collected from a single crystal.
*Data for highest resolution shell is shown in parentheses.

Supplementary Table 3. Molecular basis for disease in FED and FLD mutations

Mutation	Clinical phenotype	α LCAT activity	β LCAT activity	Ref.	Explanation
Suspected Folding/Processing Defects					
V28M	FLD (CH with A211T)	na	na	1	Disruption of packing in core of catalytic domain.
D77N	FLD (CH with T106A)	na	na	2	Loss of salt bridge between Asp^{77} and Lys^{42}.
V90M	NC	na	na	3	Disrupts packing between membrane-binding and cap domain.
S91P	FED (CH with A141T)	↓↓↓ (inv;rH)	↓↓↓ (inv;LDL)	4,5	Disrupts secondary structure of the b4-b5 hairpin in membrane binding domain.
A93T	FLD (HZ with R158C)	↓↓↓ (inv;rH)	↓↓↓ (inv;LDL)	6-8	Potentially disrupts salt bridge between Asp^{77} and Lys^{42}.
R99C	FED	↓↓↓ (inv;rH)	↓↓↓ (inv;LDL)	9	Loss of salt bridge with Glu^{35} and of stacking interaction with Phe^{57}.
T106A	FLD (CH with D77N)	na	na	2	Loss of hydrophobic interactions with Val^{125} and Arg^{135}, and of hydrogen bond with Glu^{110}.
E110D	NCh	↓↓↓ (inv;rH;NC)	na	10	Possible structural defect. Loss of salt bridge with His^{122} and Arg^{135} (residues conserved in LPLA2).
Y111N	NCh	↓↓↓ (inv;rH;NC)	na	10	Disrupts packing interactions with αA-αA′ loop (Fig. 5).
R135Q	FED (CH with P10Q)	↓↓↓ (inv;rH)	↓↓↓ (inv;LDL)	11	Loss of salt bridge with Glu^{110}.*
R135W	FLD (CH with Q347T and 416Ter)	↓↓↓ (inv;rH)	↓↓↓ (inv;LDL)	7,8	Loss of salt bridge with Glu^{110}. Possible altered solubility due to introduction of a solvent exposed hydrophobic residue.*
R140H	INT (CH with G71R)	↓↓↓ (inv;rH)	↓↓↓ (inv;LDL)	12	Histidine likely incompatible with packing.*
R140C	FLD	↓↓↓ (inv;rH;NC)	na	13	Cysteine cannot fully reproduce packing interactions of arginine
A141T	FED (CH with S91P)	↓↓↓ (inv;rH)	wt (inv;LDL)	4,5	Destabilization of catalytic domain via introduction of a larger side chain. May perturb structure only locally such that it retains binding to LDL particles.
Y144C	FED (CH with T123I)	↓↓↓ (PL;DPL)	↓ (PL;CER)	14	Creation of cavity due to shorter cysteine side chain.
R147W	FLD	↓↓↓ (inv;rH)	↓↓↓ (inv;LDL)	4,5	Loss of salt bridge to Asp^{145} and introduction of steric clashes between catalytic and membrane binding domains. *
Y156N	FLD (CH with Y83Ter)	↓↓ (inv;rH)	↓↓↓	15,16	Creation of cavity due to shorter asparagine side chain.*
G179R	FLD	↓↓↓	na	17	Introduction of steric clashes and charge via larger charged side chain.
G183S	FLD	↓↓↓	na	18	Mutation interferes with nucleophilic elbow folding and/or catalytic activity.*
L209P	FLD	na (inv;NP)	na (inv;NP)	7,8	Pro substitution perturbs secondary structure in β4 strand.*
A211T	FLD (CH with V28M)	na	na	1	Destabilization by introduction of steric clashes.
R244C	FLD (CH with L32P)	na	na	19	Loss of hydrogen bonds and packing interactions.
R244H	FED	0 (inv;rH)	wt (inv;LDL)	4	Loss of hydrogen bonds and packing interactions.
T274A	FED	↓↓↓	wt	5	Glycosylation defect (alteration in NxT consensus).

	(FLD symptoms) (CH with Y83Ter)	(PL;rH)	(PL;CER)		Likely structural defect.
T274I	FLD	↓↓↓ (inv;rH)	↓↓↓ (inv;LDL)	4,5	Glycosylation defect (alteration in NxT consensus). Likely structural defect.
M293R	FLD	na	na	20	Disrupts packing between cap domain and b4-b5 hairpin of membrane binding domain.
M293I	FLD	↓↓↓ (inv;rH)	↓↓↓ (inv;CER)	16,21	Disrupts packing between cap domain and b4-b5 hairpin of membrane binding domain.
P307S	FLD (CH with T13M)	na	na	22	Loss of packing interactions.
V309M	FLD	↓↓↓ (inv;rH)	↓↓↓ (inv;LDL)	4	Introduction of steric clashes via larger side chain.
C313Y	FLD	na (inv;NP)	na (inv;NP)	23	Loss of disulfide bridge between β7 and αE in catalytic domain.
L314F	FED (CH with R323C)	↓↓ (inv;rH)	na	10	Introduction of steric clashes via larger side chain.
L372R	FLD	↓↓↓ (inv;rH)	↓↓↓ inv;LDL)	4	Introduction of steric clashes via larger side chain.
Catalytic and/or Substrate Binding Defects					
G30S	FLD	↓↓↓ (inv;rH)	na	24,25	Disruption of oxyanion hole.
L32P	FLD	na	na	19	Disruption of oxyanion hole; likely packing defect.
G33R	FLD (CH w/ 30 bp ins)	↓↓↓ (PL;rH)	↓↓↓ (PL;CER)	26	Structural defect as well as occlusion of track B (phospholipid and cholesterol binding defect).
W75R	INT	na	na	19	Introduction of charge into track A and possible membrane binding domain destabilization.
W75S	FED (CH with T123I)	↓↓↓ (inv;rH;NC)	na	10	Modulation of track A and possible membrane binding domain destabilization.
S181N	FLD (CH with a frame shift)	↓↓↓ (inv;rH)	↓↓↓ (inv;LDL)	4,5,27	Loss of nucleophilic serine essential for catalysis.
K218N	FLD	↓↓↓ (inv;rH)	↓↓↓ (inv;LDL)	4,5	Loss of residue proposed to be involved in binding phospholipid head group (cf. LPLA2-Lys^{202}).
N228K	FLD	↓↓↓ (inv;rH)	↓↓↓ (inv;CER)	16,21,28	Possible structural defect in lid loop and defects in substrate binding.
G230R	FLD	↓↓↓ (inv;rH;NC)	na	29	Possible defects in substrate binding (cf. LPLA2-Arg^{214})
M252K	FLD	↓↓↓ (PL;rH)	na	30	Introduction of a charged residue into track A.
T321M	FLD	na (inv;NP)	na (inv;NP)	7,8	Introduction of steric clashes via larger side chain and disruption of loop bearing triad residue Asp^{345}.
G344S	FLD	na (inv;NP)	na (inv;NP)	31	Introduction of steric clashes via larger side chain.*
T347M	FED (CH with T123I)	↓↓↓ (inv;rH)	↓↓↓ (inv;LDL)	8,16,32	Mutates position likely involved in coordination of phospholipid head group (cf. LPLA2-Thr^{329}); inhibition of substrate binding.*
HDL and LDL Binding Defects					
V46E	FED	↓↓↓ (inv;rH)	↓ (inv;CER)	5,33	Destabilization likely via electrostatic repulsion with D73 and D77.
G71R	INT (CH with R140H)	↓↓↓ (inv;rH)	↓↓↓ (inv;LDL)	12	Disruption of membrane binding interface.
T123I	FED	↓↓↓ (inv;rH)	wt (inv;LDL)	8,14,32,34,35	Putative ApoA-I binding site.*

N131D	FED	↓↓↓ (inv;rH)	↓↓ (inv;LDL)	36	Putative ApoA-I binding site.*
F382V	FLD (CH with T321M)	↓↓ (PL;rH;NP)	↓↓↓ (PL;CER ;NP)	37	Putative ApoA-I binding site based on its position. Unclear why b-LCAT activity is also affected.
N391S	FED (CH with M252K)	↓↓↓ (inv;rH)	wt (inv;LDL)	38,39	Putative ApoA-I binding site.*
Ambiguous					
R158C	FLD (HZ with A93T)	↓↓ (inv;rH)	wt (inv;LDL)	6,8,16	Possible loss of favorable electrostatic interactions with Glu^{154} and Glu^{155}, or loss of activity due to side chain oxidation.
R323C	FED (CH with L314F)	↓ (inv;rH)	na	10	Possible loss of activity due to side chain oxidation.

Rows of the table are shaded according to the domain assignment of each position (see Figure 1): α/β hydrolase domain (yellow), membrane binding domain (light pink), or cap domain (light purple). CER, plasma cholesterol esterification rate (therefore represents both α and β LCAT activities); CH, compound heterozygous; DPL, assay on LDL/VLDL depleted plasma; HZ, homozygous, both mutation occur on a single allele; INT, intermediate phenotype; inv, expressed *in vitro*; LDL, assay on isolated ApoB-containing lipoproteins; na, not assayed; NC, no control for LCAT expression level; NCh, phenotype was not characterized; NP, undetectable or low protein level**;** PL, assay using patient's plasma; rH, assay on recombinant HDL proteoliposomes; wt, activity comparable to wild type LCAT; α LCAT activity, activity on HDL particles; β LCAT activity, activity on ApoB containing lipoproteins.
↓, ↓↓ and ↓↓↓ correspond to mild, medium and severe reduction in LCAT activity, respectively.
*Similar explanations for these variants were proposed using models of the catalytic core built by threading algorithms [40,41].

Supplementary References

1. Weber, C. L., Frohlich, J., Wang, J., Hegele, R. A. & Chan-Yan, C. Stability of lipids on peritoneal dialysis in a patient with familial LCAT deficiency. *Nephrol. Dial. Transplant.* **22,** 2084–2088 (2007).
2. Aranda, P. *et al.* Therapeutic management of a new case of LCAT deficiency with a multifactorial long-term approach based on high doses of angiotensin II receptor blockers (ARBs). *Clin. Nephrol.* **69,** 213–218 (2008).
3. Cohen, J. C. *et al.* Multiple rare alleles contribute to low plasma levels of HDL cholesterol. *Science* **305,** 869–872 (2004).
4. Calabresi, L. *et al.* Functional lecithin: cholesterol acyltransferase is not required for efficient atheroprotection in humans. *Circulation* **120,** 628–635 (2009).
5. Calabresi, L. *et al.* The molecular basis of lecithin:cholesterol acyltransferase deficiency syndromes: a comprehensive study of molecular and biochemical findings in 13 unrelated Italian families. *Arterioscler. Thromb. Vasc. Biol.* **25,** 1972–1978 (2005).
6. Hill, J. S., O, K., Wang, X. & Pritchard, P. H. Lecithin:cholesterol acyltransferase deficiency: identification of a causative gene mutation and a co-inherited protein polymorphism. *Biochim. Biophys. Acta* **1181,** 321–323 (1993).
7. Funke, H. *et al.* Genetic and phenotypic heterogeneity in familial lecithin: cholesterol acyltransferase (LCAT) deficiency. Six newly identified defective alleles further contribute to the structural heterogeneity in this disease. *J. Clin. Invest.* **91,** 677–683 (1993).
8. Qu, S. J., Fan, H. Z., Blanco-Vaca, F. & Pownall, H. J. In vitro expression of natural mutants of human lecithin:cholesterol acyltransferase. *J. Lipid Res.* **36,** 967–74 (1995).
9. Blanco-Vaca, F. *et al.* Molecular basis of fish-eye disease in a patient from Spain. Characterization of a novel mutation in the LCAT gene and lipid analysis of the cornea. *Arterioscler. Thromb. Vasc. Biol.* **17,** 1382–1391 (1997).
10. Holleboom, A. G. *et al.* High prevalence of mutations in LCAT in patients with low HDL cholesterol levels in The Netherlands: identification and characterization of eight novel mutations. *Hum. Mutat.* **32,** 1290–1298 (2011).
11. Kuivenhoven, J. A. *et al.* Two Novel Molecular Defects in the LCAT Gene Are Associated With Fish Eye Disease. *Arterioscler. Thromb. Vasc. Biol.* **16,** 294–303 (1996).
12. Hörl, G. *et al.* Compound heterozygosity (G71R/R140H) in the lecithin:cholesterol acyltransferase (LCAT) gene results in an intermediate phenotype between LCAT-deficiency and fish-eye disease. *Atherosclerosis* **187,** 101–109 (2006).
13. Steyrer, E. *et al.* A single G to A nucleotide transition in exon IV of the lecithin: cholesterol acyltransferase (LCAT) gene results in an Arg140 to His substitution and causes LCAT-deficiency. *Hum. Genet.* **96,** 105–109 (1995).
14. Contacos, C., Sullivan, D. R., Rye, K. A., Funke, H. & Assmann, G. A new molecular defect in the lecithin: cholesterol acyltransferase (LCAT) gene associated with fish eye disease. *J. Lipid Res.* **37,** 35–44 (1996).
15. Klein, H. G. *et al.* Two different allelic mutations in the lecithin:cholesterol acyltransferase (LCAT) gene resulting in classic LCAT deficiency: LCAT (tyr83→

stop) and LCAT (tyr156→ asn). *J. Lipid Res.* **34,** 49–58 (1993).
16. Klein, H. G. *et al.* In vitro expression of structural defects in the lecithin-cholesterol acyltransferase gene. *J. Biol. Chem.* **270,** 9443–9447 (1995).
17. Wang, X. L. *et al.* Molecular analysis of a novel LCAT mutation (Gly179 → Arg) found in a patient with complete LCAT deficiency. *J. Atheroscler. Thromb.* **18,** 713–719 (2011).
18. McLean, J. Molecular defects in the lecithin:cholesterol acyltransferase gene. *In High density lipoproteins and atherosclerosis III* (Miller, N. E. & Tall, A. R.) 59–65 (1992).
19. Charlton-Menys, V. *et al.* Molecular characterization of two patients with severe LCAT deficiency. *Nephrol. Dial. Transplant.* **22,** 2379–2382 (2007).
20. Roshan, B. *et al.* Homozygous lecithin:cholesterol acyltransferase (LCAT) deficiency due to a new loss of function mutation and review of the literature. *J. Clin. Lipidol.* **5,** 493–499 (2011).
21. Gotoda, T. *et al.* Differential phenotypic expression by three mutant alleles in familial lecithin:cholesterol acyltransferase deficiency. *Lancet* **338,** 778–781 (1991).
22. Argyropoulos, G. *et al.* Transmission of two novel mutations in a pedigree with familial lecithin:cholesterol acyltransferase deficiency: structure-function relationships and studies in a compound heterozygous proband. *J. Lipid Res.* **39,** 1870–1876 (1998).
23. Holleboom, A. G. *et al.* Proteinuria in early childhood due to familial LCAT deficiency caused by loss of a disulfide bond in lecithin:cholesterol acyl transferase. *Atherosclerosis* **216,** 161–165 (2011).
24. Rosset, J., Wang, J., Wolfe, B. M., Dolphin, P. J. & Hegele, R. A. Lecithin:cholesterol acyl transferase G30S: association with atherosclerosis, hypoalphalipoproteinemia and reduced in vivo enzyme activity. *Clin. Biochem.* **34,** 381–386 (2001).
25. Yang, X. P. *et al.* Catalytically inactive lecithin: cholesterol acyltransferase (LCAT) caused by a Gly 30 to Ser mutation in a family with LCAT deficiency. *J. Lipid Res.* **38,** 585–591 (1997).
26. Wiebusch, H. *et al.* Deficiency of lecithin:cholesterol acyltransferase due to compound heterozygosity of two novel mutations (Gly33Arg and 30 bp ins) in the LCAT gene. *Hum. Mol. Genet.* **4,** 143–145 (1995).
27. Frascà, G. M. *et al.* A 33-year-old man with nephrotic syndrome and lecithin-cholesterol acyltransferase (LCAT) deficiency. Description of two new mutations in the LCAT gene. *Nephrol. Dial. Transplant.* **19,** 1622–1624 (2004).
28. Adimoolam, S., Jin, L., Grabbe, E., Shieh, J. J. & Jonas, A. Structural and functional properties of two mutants of lecithin-cholesterol acyltransferase (T123I and N228K). *J. Biol. Chem.* **273,** 32561–32567 (1998).
29. Miettinen, H. E. *et al.* Molecular Genetic Study of Finns With Hypoalphalipoproteinemia and Hyperalphalipoproteinemia : A Novel Gly230Arg Mutation (LCATFin) of Lecithin:Cholesterol Acyltransferase (LCAT) Accounts for 5% of Cases With Very Low Serum HDL Cholesterol Levels. *Arterioscler. Thromb. Vasc. Biol.* **18,** 591–598 (1998).
30. Skretting, G., Blomhoff, J. P., Solheim, J. & Prydz, H. The genetic defect of the

original Norwegian lecithin:cholesterol acyltransferase deficiency families. *FEBS Lett.* **309,** 307–310 (1992).
31. Moriyama, K. *et al.* Two novel point mutations in the lecithin:cholesterol acyltransferase (LCAT) gene resulting in LCAT deficiency: LCAT (G873 deletion) and LCAT (Gly344→ Ser). *J. Lipid Res.* **36,** 2329–2343 (1995).
32. Klein, H. G. *et al.* Two different allelic mutations in the lecithin-cholesterol acyltransferase gene associated with the fish eye syndrome. Lecithin-cholesterol acyltransferase (Thr123→ Ile) and lecithin-cholesterol acyltransferase (Thr347→Met). *J. Clin. Invest.* **89,** 499–506 (1992).
33. Calabresi, L. & Francheschini, G. “Genetic LCAT deficiency: molecular diagnosis, plasma lipids, and atherosclerosis.” In *High Density Lipoproteins, Dyslipidemia, and Coronary Heart Disease* (Editor Schaefer, E. J.) pp. 89–93 (Springer New York, 2010).
34. O, K., Hill, J. S., Wang, X. & Pritchard, P. H. Recombinant lecithin: cholesterol acyltransferase containing a Thr123 → Ile mutation esterifies cholesterol in low density lipoprotein but not in high density lipoprotein. *J. Lipid Res.* **34,** 81–88 (1993).
35. Funke, H. *et al.* A molecular defect causing fish eye disease: an amino acid exchange in lecithin-cholesterol acyltransferase (LCAT) leads to the selective loss of alpha-LCAT activity. *Proc. Natl. Acad. Sci. USA* **88,** 4855–4859 (1991).
36. Kuivenhoven, J. A. *et al.* A unique genetic and biochemical presentation of fish-eye disease. *J. Clin. Invest.* **96,** 2783–2791 (1995).
37. Nanjee, M. A novel LCAT mutation (Phe382→Val) in a kindred with familial LCAT deficiency and defective apolipoprotein B-100. *Atherosclerosis* **170,** 105–113 (2003).
38. Rader, D. J. *et al.* Markedly accelerated catabolism of apolipoprotein A-II (ApoA-II) and high density lipoproteins containing ApoA-II in classic lecithin: cholesterol acyltransferase deficiency and fish-eye disease. *J. Clin. Invest.* **93,** 321–330 (1994).
39. Vanloo, B. *et al.* Relationship between structure and biochemical phenotype of lecithin:cholesterol acyltransferase (LCAT) mutants causing fish-eye disease. *J. Lipid Res.* **41,** 752–761 (2000).
40. Peelman, F. *et al.* A proposed architecture for lecithin cholesterol acyl transferase (LCAT): identification of the catalytic triad and molecular modeling. *Protein Sci.* **7,** 587–99 (1998).
41. Peelman, F. *et al.* Effects of natural mutations in lecithin:cholesterol acyltransferase on the enzyme structure and activity. *J. Lipid Res.* **40,** 59–69 (1999).